A MODEL OF LOOPS IN 2D*

Aleix Prats

Departament d'Estructura i Constituents de la Materia
Facultat de Física, Universitat de Barcelona
Diagonal 647, 08028 Barcelona, Spain

(Received August 13, 2003)

The gonihedric spin model was first introduced as the action for a discretized tensionless string in a discretized embedding space. Afterwards was found that there are interesting features on the dynamical behavior of this model in 3 dimensions (as it was first formulated) that make us think on glassy spin model without inherent disorder. Extensive simulations have been carried out in the 3-dimensional model. In the following I will report on a work composed of two different but related parts. The first part is a numerical study through Monte Carlo simulations of the dynamical properties of the 2 dimensional version of the model (*i.e.* the loop model), which is much simpler due to the fact that it has trivial thermodynamical properties. The second part consists on an analytical approach of this 2-dimensional loop model coupled to gravity. We solve partially the associated two-matrix model via a reduction to an equivalent one matrix model and saddle point methods with the last one-matrix model.

PACS numbers: 75.10.Hk, 68.35.Ja, 04.60.Nc, 04.60.Kz

1. Statistical model of loops in 2D

The gonihedric spin model was first introduced by Savvidy in relation to a discretized model for a tensionless string theory [1], but very soon the spin model gained interest by itself. Also its extension to a self-interacting surfaces ($\kappa \neq 0$) showed a very rich family of models with different kind of critical points and interesting dynamical properties [1–3]. Extensive numerical and theoretical work appeared [4–7] and some interest about the glassiness of the 3-dimensional gonihedric model arosen [8–12]. This is precisely the aspect of the model that has motivated us to study the 2-dimensional

* Presented at the Workshop on Random Geometry, Kraków, Poland, May 15–17, 2003.

version of the model. Its trivial thermodynamics motivates us to investigate whether this model also has glassy behavior or not. This would provide a toy model for glassy phenomena without inherent disorder on the couplings.

So the spin model we are going to investigate is related to a model of loops in 2 dimensions. We are going to compare this model and the results we obtained from analogous simulations in a 3-dimensional version of this spin model [12]. But before we go into the analysis of the model let us define it in terms of spin variables.

Consider the following Hamiltonian

$$\mathcal{H}^{\mathrm{2D}}_{\mathrm{gonih}} = -\kappa \sum_{\langle i,j\rangle} \sigma_i\sigma_j + \frac{\kappa}{2} \sum_{\langle\langle i,j\rangle\rangle} \sigma_i\sigma_j + \frac{1-\kappa}{2} \sum_{[i,j,k,l]} \sigma_i\sigma_j\sigma_k\sigma_l \tag{1.1}$$

in a two-dimensional lattice[1], where $\langle i,j\rangle$ means sum over nearest neighbors, $\langle\langle i,j\rangle\rangle$ means sum over next to nearest neighbors, and $[i,j,k,l]$ means over spins forming plaquettes on the lattice.

This Hamiltonian has some odd characteristics. The most important of all is that the space of symmetric vacua is extremely large, in fact it is exponentially large with the dimension of the lattice L. In particular, the simultaneous flip of all the spins that belong to any set of non-crossing lines leaves the energy of the ferromagnetic ground state unchanged[2] [13]. This symmetry is even larger in the $\kappa = 0$ case where the lines can cross each other. This provides a very special landscape for the energy function of our model that in its 3-dimensional version makes the system exhibit a very clear glassy behavior associated to a thermodynamical phase transition [10]. This is precisely the aim of this work: to determine whether or not the same kind of behavior can be found in 2 dimensions given that the 2D model has no thermodynamical phase transition.

Let us first see the relation between this model and the loop model we announced. If we look at the energy of a given configuration we can see that due to the precise fine tuning of the couplings all the energy is concentrated at the bending points of the loop (surface in this 3D case) that is the boundary between the two different phases of the system (*i.e.* between plus and minus spins), and that wherever there is a crossing of this surface

[1] The 3-dimensional counterpart has slightly modified couplings. The explicit form is

$$\mathcal{H}^{\mathrm{2D}}_{\mathrm{gonih}} = -2\kappa \sum_{\langle i,j\rangle} \sigma_i\sigma_j + \frac{\kappa}{2} \sum_{\langle\langle i,j\rangle\rangle} \sigma_i\sigma_j + \frac{1-\kappa}{2} \sum_{[i,j,k,l]} .$$

The reason is that the number of neighbors changes from 3D to 2D, thus the couplings have to change too as we will argue.

[2] In the 3-dimensional case this symmetry is generated by the flip of planes rather than lines.

with itself (or with another loop) there is another concentration of extra energy. So at the end of the day we can write the energy of the spin model (or the loop model) as follows

$$E = n_2 + 4\kappa n_4 \,, \tag{1.2}$$

where n_2 is the number of bending points and n_4 the number of self-crossing points of the loop that separates the plus and minus spins regions.

This is exactly the same that happens in the 3-dimensional version of the model. In fact the couplings are precisely chosen to exhibit these features. But all this has very different consequences for 2 dimensions or 3 dimensions. The main difference between this 2D loop model and the corresponding 3D surface model is that the action of the surface in 3D is proportional to the linear extent of the surface (see Fig. 1(a)) and the roughness of it, while the action for the loop is not depending on how big it is but on how many times it bends (see Fig. 1(b)). Thus in 2 dimensions the energy of the loop do not depend on its size but on the shape of it (although the energy barriers do eventually depend on the size of the loop).

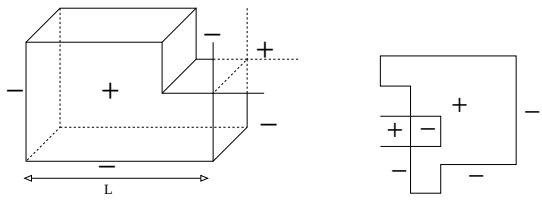

Fig. 1. Examples of configurations of the system in 3D — (a) and in 2D — (b). The energy is concentrated on the bending and crossing points (2D) and lines (3D).

1.1. Thermodynamical behavior

Let's now take a look at the thermodynamical properties of this spin model taking as a reference its 3-dimensional counterpart [5, 12]. Let us begin with the special case of $\kappa = 0$ that is exactly solvable in infinite volume and reducible to an easy-computable sum for finite volume. The exact solution for the model with $\kappa = 0$ shows us that there is no phase transition at finite temperature. If we take a look at Fig. 2 we will see the infinite volume energy function and susceptibility compared to the numerical results of simulations and to the exact finite volume calculation. All the discordances between simulations and the infinite volume calculations are due to finite volume effects as we can see comparing the simulations with the exact finite volume calculations. For the other cases with $\kappa \neq 0$ there is no infinite volume exact solution nor easy-computable finite-volume expression but the

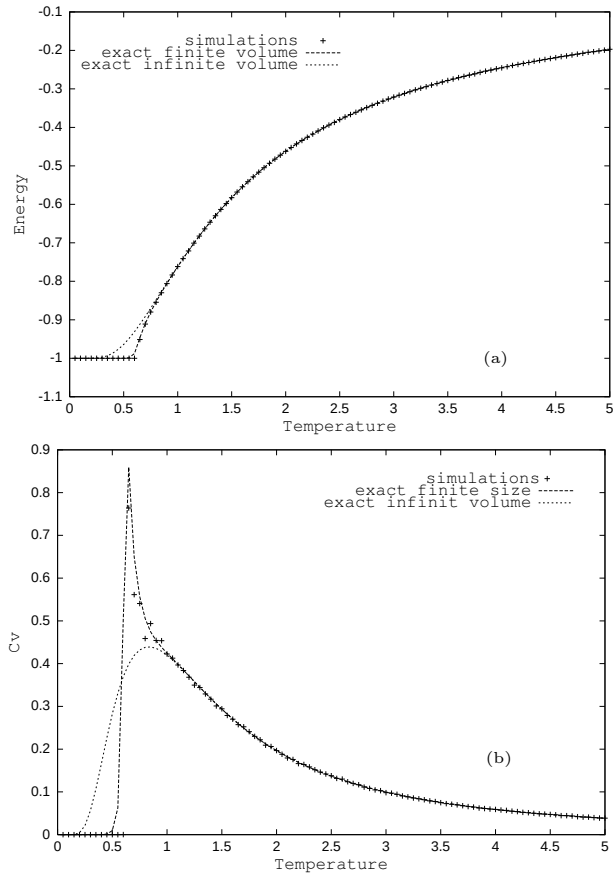

Fig. 2. (a) — energy function and (b) — specific heat of the system for $\kappa = 0$. The exact function at infinite volume, at finite volume, and the Monte Carlo simulations are plotted.

simulations performed do not show great differences with the $\kappa = 0$ case (see Fig. 3). The only remarkable difference is the appearance of a second structure for sufficiently large κ. This second structure can be interpreted as the appearance of a new energy level for the plaquette variables. This has been studied to see whether it evolves into a peak at large volumes, but no volume dependence of this structure has been found, so there is no evidence of phase transition.

On the other hand the same model in three dimensions exhibits a quite complex phase space. For $\kappa = 0$ there is a critical temperature T_c where the system changes from ordered to disordered phase through a first order phase transition, and a second temperature T_g that is between two different dy-

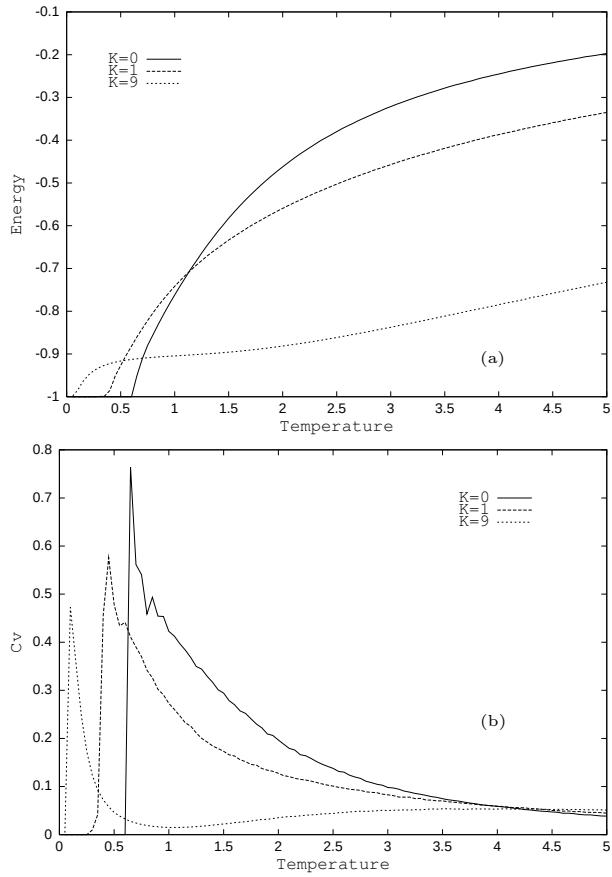

Fig. 3. (a) — energy function and (b) — specific heat of the system for $\kappa = 0$. The exact function at infinite volume and the Monte-Carlo simulations are plotted.

namical phases: a glassy phase and a supercooled phase (see Fig. 4) [9,11,14]. Increasing κ we find from certain value on that this second temperature T_{g} either is very close to the thermodynamical temperature T_{c} or they coincide, and that this thermodynamical phase transition changes from first to second order.

Thus we have seen that this models from 3 dimensions to 2 dimensions changes a lot its thermodynamical behavior. From having first/second order phase transitions (depending on the value of κ) on 3D to trivial thermodynamics without any phase transition on 2D. But we also want to know whether there is a great difference or not in they dynamical properties. In particular we want to know if the slow dynamics and the glassy behavior remains on the 2-dimensional model.

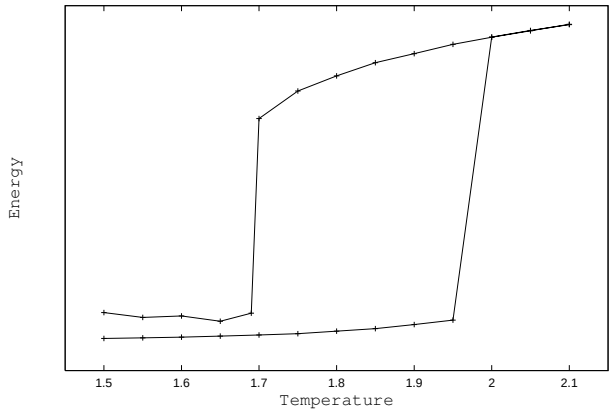

Fig. 4. Energy *versus* temperature. The lower branch is produced heating the ferromagnetic ground state. The higher branch corresponds to sudden quenches at each temperatures from disordered configurations.

1.2. Dynamical behavior

We will move now to the dynamical properties of the model. We shall report here only the $\kappa = 0$ case[3].

To study the dynamics of this system we will consider a two-time correlator of local observables [15]

$$C(t, t_{\mathrm{w}}) = \sum_i e_i(t_{\mathrm{w}}) e_i(t_{\mathrm{w}} + t)\,, \tag{1.3}$$

where the sum runs over all the sites in the lattice, and the variable $e_i(t)$ is the energy[4] of the site i at the time t. This object, in equilibrium, should be independent of t_{w}, but as we can see in Fig. 5 below some temperature this function happens to depend on the waiting time t_{w}, such observation is identical to the one made for the 3-dimensional case where an even larger dependence of this autocorrelation function on the waiting time appeared below T_{g} (see Fig. 6). This is not *per se* a clear evidence for glassy behavior of the model yet, so we will continue with the program we followed with the 3-dimensional model. Thus let us fit the curves that look t_{w}-independent (*i.e.* the curves that should be above the hypothetical glassy transition temperature T_{g}). The fitting function will be of the form

$$A\mathrm{e}^{-(t/\tau)^b} \tag{1.4}$$

[3] Due that we have not established yet without ambiguities whether this case posses or not glassy behavior we are not going to consider the $\kappa \neq 0$ case.

[4] We could have used other kind of observables like the spin variables or the energy per plaquette, but they have the same behavior for our purposes.

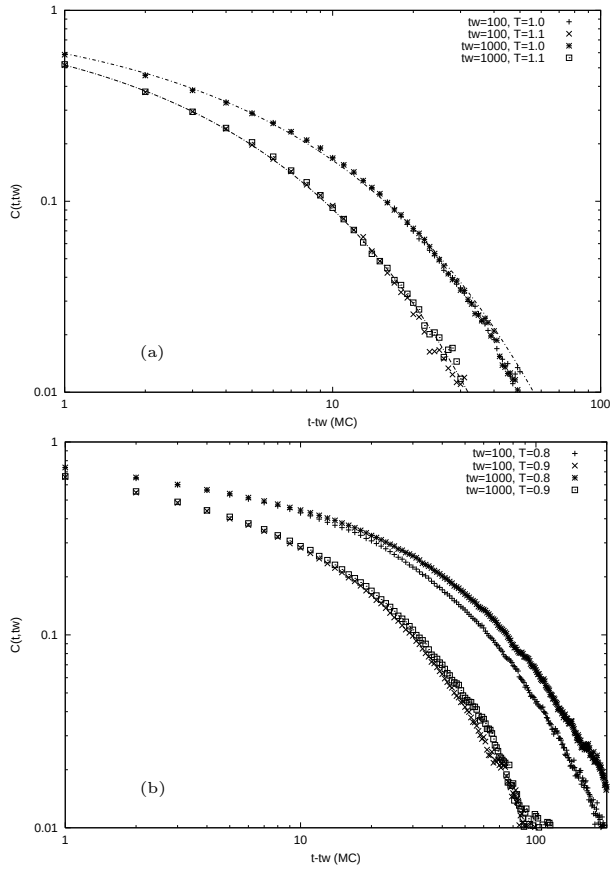

Fig. 5. Autocorrelation functions for different temperatures and different waiting times: (a) — curves are independent at $t_{\rm w}$ (b) — some dependence in $t_{\rm w}$ appears.

which is an stretched exponential. As you can see in Fig. 5(a) the agreement between the fit and the simulations is rather good[5]. Now we can plot the fitted values of τ against temperature, and we see that it increases as we lower the temperature as if it liked to diverge at some point. If we fit this points using a function of the form

$$\frac{\tau_0}{(T - T_*)^c} \tag{1.5}$$

as we did in 3 dimensions, we will find a good parameterization of the di-

[5] Lines are fits, points are simulation measurements. We looked for the consistency of the fits by checking that the true value of the parameter A, *i.e.* $A = 1$ (which we know by construction of the correlation function) were within the interval of confidence of the fitted value

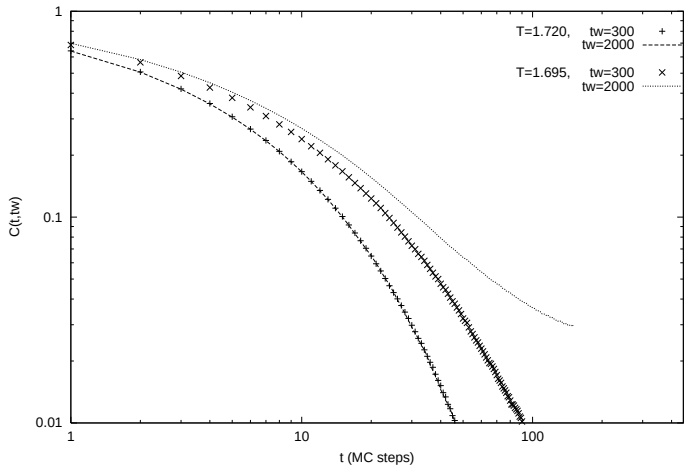

Fig. 6. Curves of autocorrelation of the spin variables at both sides of $T_{\rm g}$ on the 3-dimensional gonihedric model.

vergence (see Fig. 7) although there is still something that is not completely compatible with this fit. The problem with this fit is that the fitted "glassy" temperature T_* is not consistent with the point where the autocorrelation function began to depend on the waiting time, as it should. This is why we should analyze more carefully this autocorrelation function. Looking more carefully at this autocorrelation function we can see that the dependence in

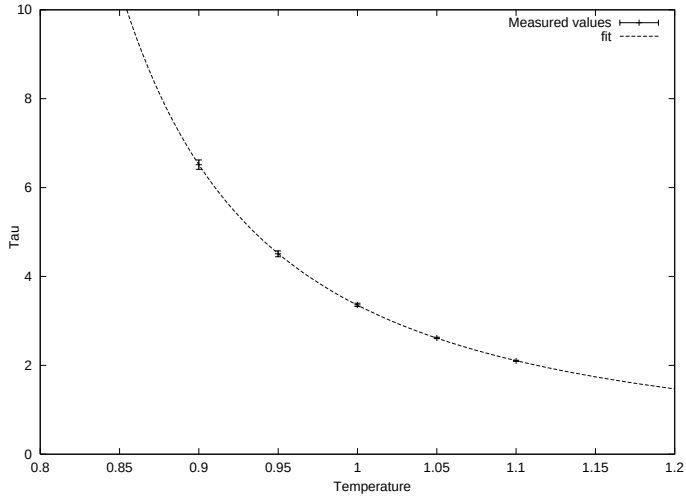

Fig. 7. Autocorrelation time *versus* temperature at temperatures above 0.9.

the waiting time t_w disappears as we increase it. This means that the thermalization of these two time functions is extremely slow, but that could be non-glassy-like. In Fig. 8 we can see this convergence of the autocorrelation functions as we increase the waiting time.

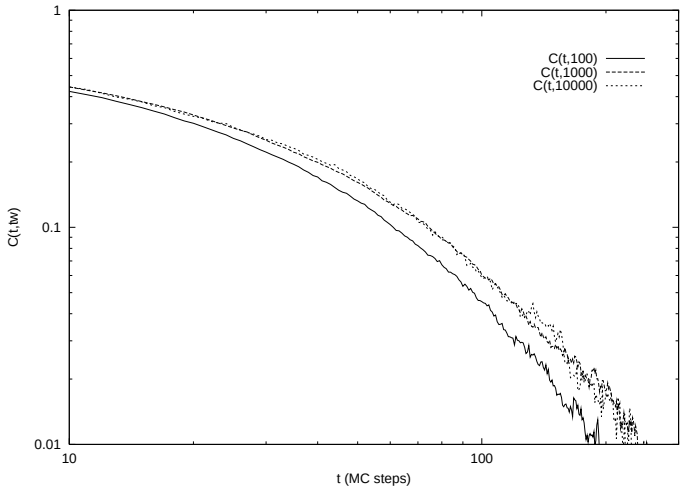

Fig. 8. Evolution of the autocorrelation function with the waiting time t_w.

To explore better the dynamics behavior of this model we can perform other type of experiments in our system. For example we can prepare our system in a specific configuration, for example a lattice with two different coexisting vacua, one inside the other (one possibility could be layer-like vacua inside ferromagnetic one) and look at the decay process of the system to the equilibrium. The problem with this tests is that as there is no ordered phase in this model, we cannot prepare the system in an initial configuration composed by two different coexisting vacua and pretend that they are more disordered than the equilibrium-like configurations at the temperatures we are examining, as it is in the 3-dimensional case (Fig. 9 shows the 3D decay of a perturbed vacua to the unperturbed one. It is easy to see the different behaviors in terms of temperature). In spite of this we performed those simulations and found that the decay behaved in the same way for all the range of temperatures (Fig. 10(a) and Fig. 10(b) are two examples of this decays at both sides of the hypothetical T_g). The magnitude we used to study this decay in two dimensions is the energy difference with the equilibrium. If we look at the value of the fitted exponent c of the function (1.4) that we have also used in this experiments, we can see that they are really close to one, and this suggests that the behavior may not be glassy but 'usual' albeit rather slow exponential decay.

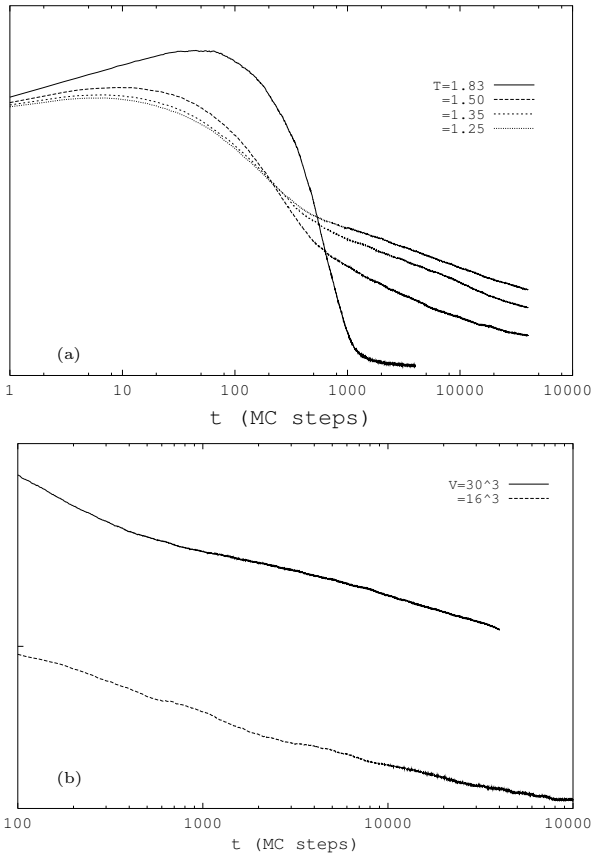

Fig. 9. In the 3D gonihedric model: (a) — evolution of some order parameter starting from a perturbed vacua as an initial configuration. We can see two kind of behaviors. In (b) we see that the low temperature behavior is logarithmic. Lines are evolutions for different initial volumes of the perturbations at a temperature deep inside low temperature region.

In the analysis of the glassiness of the system we can introduce a new observable; the Q parameter [15]. This parameter is defined in the following way: after evolving a single system t_{w} Monte Carlo steps, we make two copies of the system and let them evolve independently, then the Q of a local observable is the overlap of this observable between the two independent copies of the system. In our case we will use the local spin variables

$$Q = \sum_i \sigma_i^a(t_{\mathrm{w}} + t)\sigma_i^b(t_{\mathrm{w}} + t)\,. \tag{1.6}$$

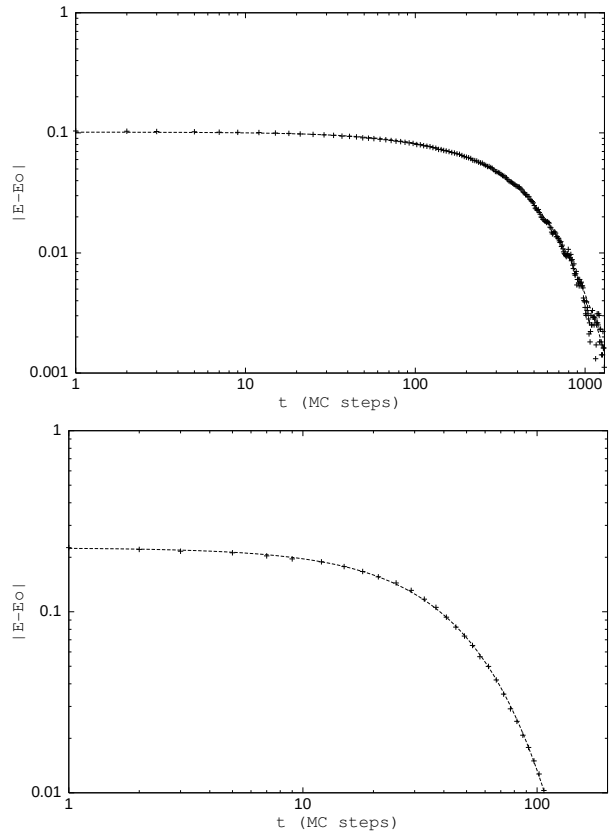

Fig. 10. The decay of a prepared initial configuration to the equilibrium.

Then, using this Q parameter and the time overlap of the same local magnitude,

$$C_{\text{spin}}(t, t_{\text{w}}) = \sum_i \sigma_i(t_{\text{w}})\sigma_i(t_{\text{w}} + t)\,, \tag{1.7}$$

we can perform different kind of analysis. One of those is the following. It is known that the system must satisfy the relation

$$C_{\text{spin}}(t_{\text{w}}, t) = Q\left(t_{\text{w}}, \frac{t}{2}\right) \tag{1.8}$$

if we are in an ordinary non-glassy phase. As we can see in Fig. 11(a) and Fig. 11(b) there are temperatures[6] for which the behavior of the Q parameter

[6] Remember that $T = 0.8$ is already a temperature where, at waiting times we are considering, the energy auto-correlators are not t_{w} independent.

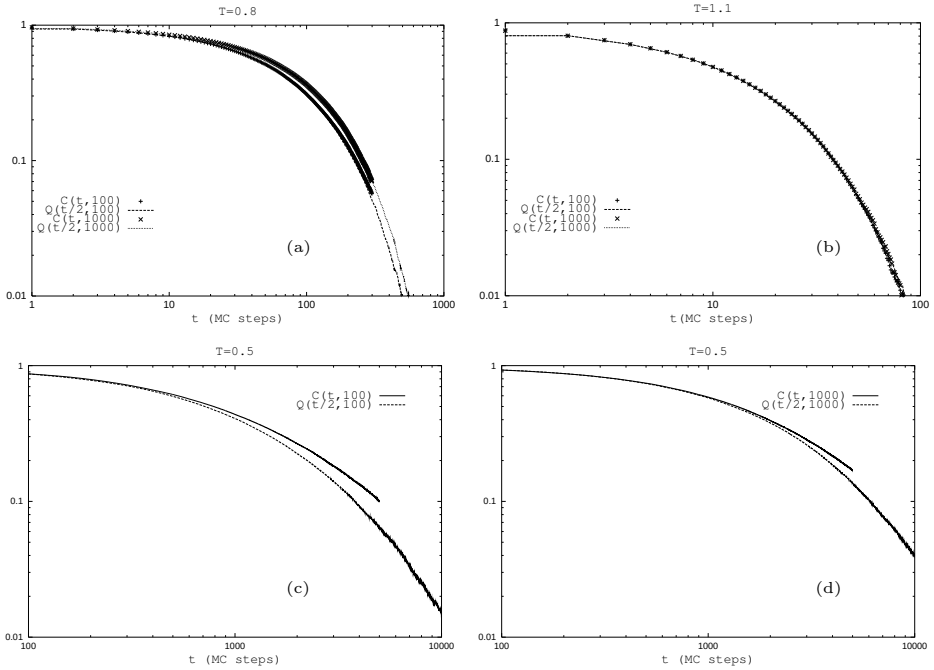

Fig. 11. Plots of the functions $C(t, t_{\rm w})$ and $Q(t/2, t_{\rm w})$ for different temperatures and different $t_{\rm w}$. In (a) and (b) we see how the scaling (1.8) is satisfied for any $t_{\rm w}$. In (c) and (d) we see that the relation of scaling is not satisfied at low temperatures.

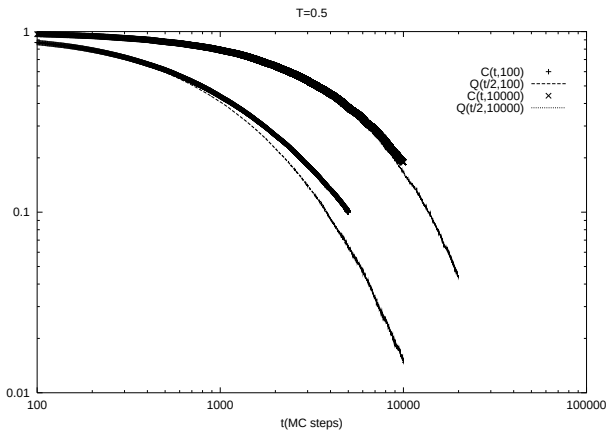

Fig. 12. The convergence to the scaling behavior is clear in this plot where $t_{\rm w}$ has been increased by one order of magnitude.

with respect to the C_{spin} two times auto-correlator is what we expected, while there are lower temperatures, like in Fig. 11(c) and Fig. 11(d) where the relation (1.8) is not satisfied at large enough times, for the value of t_{w} we simulate, although the discrepancy region is moving to larger times as we increase t_{w} as if it would like to follow (1.8) for large t_{w} (see Fig. 12).

1.3. Conclusions

At this point we have concluded the analysis of all our simulations without any clear reason to believe that this 2-dimensional version of Savvidy's gonihedric model has really glassy behavior; on the contrary it seems to exhibit only very slow dynamics not related to real glassiness of the model. This has to be further investigated to clear out what type of dynamics is this model developing. Also $\kappa \neq 0$ has to be investigated although we think it will follow the same kind of behavior that the $\kappa = 0$ case.

2. The model of loops coupled to gravity

There exist a way to extent this model to one coupled to gravity. To couple it to gravity we will put our spin model in a random lattice built from quadrangular pieces. In this way we will keep the behavior of the loops and add the gravity degrees of freedom. In order to make the matrix model solvable (or approximately solvable) we will make the loops highly self-interacting, that means that the loops will never cross themselves. This corresponds to the $\kappa \to \infty$ limit in the model we presented above. In Fig. 13 we can see an example of this kind of quadrangulations. From this picture we can extract the weights of each interaction term in the matrix model that will represent the partition function of our system. Let us see what those terms mean.

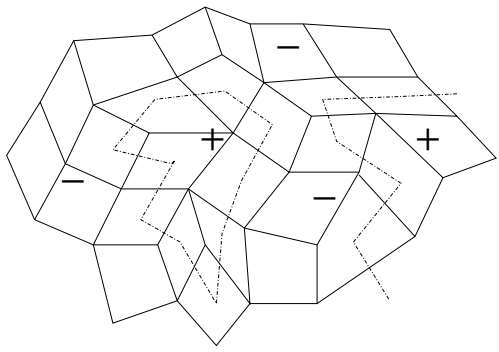

Fig. 13. Example of a random lattice with a gonihedric spin model on it.

First of all there will be the bulk term (in other words, plaquette that is not crossed by any loop), then we have to consider a term were a plaquette is crossed by one loop without bending through it and finally the term were the loop crossing the plaquette bends in one direction or the other. These three building blocks of the random lattices are presented graphically in Fig. 14 with the corresponding term of the matrix model that will generate them[7]. As we can see we are considering the most general case where all the

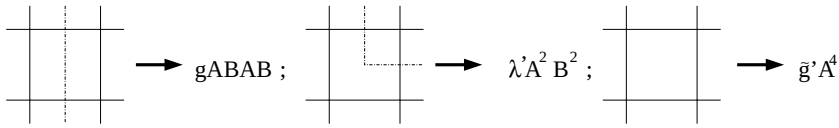

Fig. 14. Correspondence between the loop pieces and the matrix interaction that are going to generate them.

couplings are different but in our specific case we will impose the condition $\tilde{g} = g$ due to the fact that a straight piece of loop do not contribute with any amount of energy to the action, so the coupling has to be equal to the bulk coupling. In addition to those terms we have to put the kinetic term for the two matrices, *i.e.* the quadratic terms A^2 and B^2. So finally the matrix model that will represent our loop model coupled to gravity will be

$$\mathrm{e}^Z = \iint dA dB \exp\left(-\operatorname{Tr}\left[A^2 + B^2 + \frac{g}{N}A^4 + \frac{\lambda'}{N}A^2B^2 + \frac{\tilde{g}'}{N}ABAB\right]\right). \tag{2.1}$$

Now that we have found the matrix model that will reproduce our loop model coupled to gravity we only need to develop its solution. To our knowledge this model has not been solved exactly. Although very similar matrix models have been indeed solved [16] their solution cannot be applied to our matrix model.

2.1. A partial solution to the matrix model

Let us proceed then to the approximation to the solution. To this aim we are going to rescale the A matrix in the form $A \to \sqrt{\frac{N}{g}}A$ so that the action will have the following appearance.

$$S = \frac{N}{g}\operatorname{Tr}[A^2 + A^4] + \operatorname{Tr}[B^2 + \lambda A^2B^2 + \tilde{g}ABAB]\,, \tag{2.2}$$

[7] To simplify the visual identification with the loop model we have not drawn the lines corresponding to the "bulk" propagator, *i.e.* to the A matrix propagator. The loop is generated with the B matrix propagator.

where we have made some redefinitions like $\lambda'/g \to \lambda$ and $\tilde{g}'/g \to \tilde{g}$. Now we are going to pay attention to the B–dependent part. As the action S is quadratic in B we should be able to integrate out the B matrix and find a one matrix model equivalent to the one we are using now.

The integration we are facing now is the following

$$\int dB \ \exp\left(- \mathrm{Tr}[B(\mathbb{I} + \lambda A^2)B] - \tilde{g} \ \mathrm{Tr}[ABAB]\right). \tag{2.3}$$

Here we are going to interpret the first part of the action as the free action (and rename $\mathbb{I} + \lambda A^2 = M$) and the second part as the interaction, so we can do perturbation theory and re-sum all the diagrams at the end. But before we calculate diagrams we need to know the free propagator of the B matrix, and to reach this we add some external currents and perform the quadratic integration[8]. So finally we find the propagator

$$\langle B_{ij} B_{kl} \rangle = \tilde{Z}(0, M) \left[\frac{\mathbb{I} \otimes \mathbb{I}}{\mathbb{I} \otimes M + M \otimes \mathbb{I}} \right]_{il;kj}, \tag{2.4}$$

where $\tilde{Z}(0, M)$ a determinant coming from the B integration. Once we have found the propagator we can proceed with the diagrammatic. We will only consider the connected diagrams. The Feynman rules for the diagrams will be those shown in Fig. 15. To order n in the interaction term there

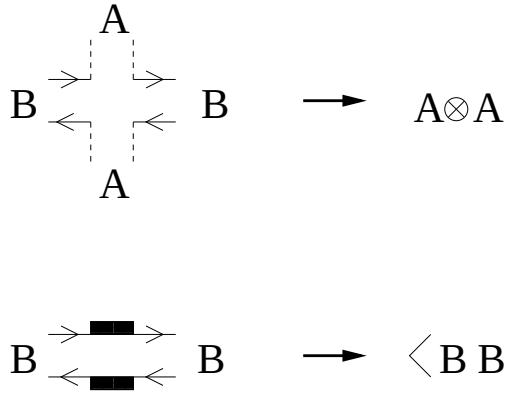

Fig. 15. Feynman rules for our matrix model.

will be also a factor $-\tilde{g}/n!$ due to the expansion of the exponential, and a combinatorial factor of $(n-1)!\ 2^{n-1}$ coming from the reordering of the interaction terms (in Fig. 16 we can see the kind of diagrams that will contribute). So finally all connected diagrams add up to

[8] In Appendix A is shown in detail how to make this calculation and find $\tilde{Z}(J, M)$.

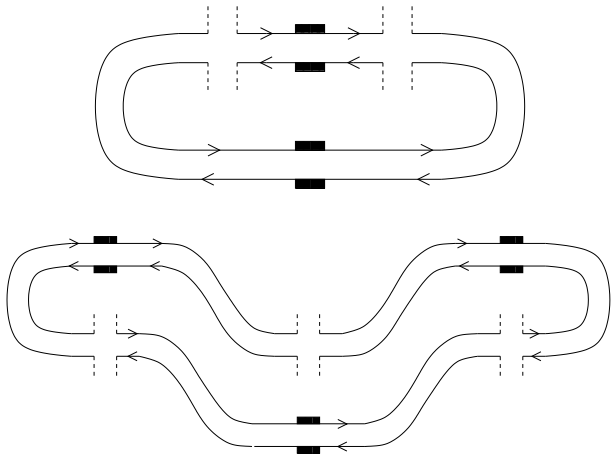

Fig. 16. Two examples of connected diagrams that contribute to the integral. a non trivial contraction is shown in the second diagram, can be easily seen that is exactly equivalent to the trivial diagram.

$$\begin{aligned}
&\sum_{n=1}^{\infty} \frac{(-\tilde{g})^n\ (n-1)!\ 2^{n-1}}{n!} \operatorname{Tr}\left[(A\otimes A\ [\mathbb{I}\otimes M + M\otimes\mathbb{I}]^{-1})^n\right] \\
&\quad = \operatorname{Tr}\left[\frac{1}{2}\sum_{n=1}^{\infty}\frac{(-2\tilde{g})^n}{n}\Big(A\otimes A[\mathbb{I}\otimes M + M\otimes\mathbb{I}]^{-1}\Big)^n\right] \\
&\quad = \frac{-1}{2}\operatorname{Tr}\left[\log\left(\mathbb{I}\otimes\mathbb{I} + \frac{2\tilde{g}A\otimes A}{2\mathbb{I}\otimes\mathbb{I} + \lambda(\mathbb{I}\otimes A^2 + A^2\otimes\mathbb{I})}\right)\right],
\end{aligned}$$

where we have recovered the explicit form of M in terms of A. Thus exponentiating this last expression we recover all connected and disconnected diagrams; *i.e.* the integral (2.3) we were trying to calculate.

$$\begin{aligned}
&\int dB\ \exp\left(-\operatorname{Tr}[B(\mathbb{I}+\lambda A^2)B]\ -\tilde{g}\operatorname{Tr}[ABAB]\right) \\
&= \tilde{Z}(0,M)\exp\left\{\frac{-1}{2}\operatorname{Tr}\left[\log\left(\mathbb{I}\otimes\mathbb{I} + \frac{2\tilde{g}A\otimes A}{2\mathbb{I}\otimes\mathbb{I} + \lambda(\mathbb{I}\otimes A^2 + A^2\otimes\mathbb{I})}\right)\right]\right\}.
\end{aligned}$$

So finally we have found an expression for the integration of the B matrix. In this expression $\tilde{Z}(0,M) = [\det(\mathbb{I}+\lambda A^2)]^{-\frac{N}{2}}$ that can be included in the effective action as $-\frac{N}{2}\operatorname{Tr}[\log(\mathbb{I}+\lambda A^2)]$. This means that we have rewritten our two matrix model in terms of a one matrix model. So now we can diagonalize our remaining A matrix and integrate over the rotational degrees

of freedom to leave our partition function in the form

$$\begin{aligned} \mathrm{e}^{Z} &= \iint dA dB \exp\left(-\mathrm{Tr}[A^2+B^2+\tilde{g}'A^4+\lambda A^2B^2+g'ABAB]\right) \\ &= \int \left(\prod_{i=1}^{N} da_i\right)\Delta^2(a)\exp\left\{-\frac{N}{\tilde{g}}S_{\mathrm{eff}}(\{a\})\right\}, \end{aligned}$$

where $\Delta(a)=\prod_{i<j}(a_j-a_i)$ is the usual Van der Monde determinant and S_{eff} is the following

$$\begin{aligned} S_{\mathrm{eff}}(\{a\}) &= \sum_{i=1}^{N}\left(a_i^2+a_i^4+\frac{g}{2}\log(1+\lambda a_i^2)\right) \\ &\quad +\sum_{i,j}^{N}\frac{\tilde{g}}{2N}\log\left(1+\frac{2\tilde{g}a_ia_j}{2+\lambda(a_i^2+a_j^2)}\right). \end{aligned}$$

Since we are working in terms of eigenvalues we can use standard procedures to try to solve the model. Using saddle point approximation we arrive to a set of coupled equations that look quite difficult to solve exactly. In the $N\to\infty$ limit those equations read

$$\begin{aligned} &a+4a^3+g\left[\frac{\lambda a}{1+\lambda a^2}+\int db\rho(b)\frac{2\tilde{g}b(2+\lambda(b^2-a^2))}{(2+\lambda(b^2+a^2)+2\tilde{g}ba)(2+\lambda(b^2+a^2))}\right] \\ &\quad = 2g\fint db\frac{\rho(b)}{a-b} = -g(\omega(a+i\epsilon)+\omega(a-i\epsilon)), \end{aligned}$$

where as usual $\rho(a)=\lim_{N\to\infty}\left[\frac{1}{N}\Sigma_{i=1}^{N}\delta(a-a_i)\right]$ and the resolvent $\omega(z)$ is defined to be equal to $\int db\ \rho(b)/(b-z)$. This self-consistent equation has to be analyzed carefully to see whether there is any fixed point in the set of parameters that allowed us to pas to the continuum.

2.2. Conclusions

In the conclusions of this second part we may comment that, since the fixed geometry model we have studied in the first part does not posses any thermodynamical singularity, even for $\kappa\to\infty$, we would naively expect the present matrix model not to exhibit any scaling limit, but this issue deserves further analysis. Related to this matrix model there are other matrix models that can be exactly solved [16]. Although those other models have some critical differences, their solutions may give some hints on how to exactly solve the model we are interested in. In fact some of the solved models can be found as an special limit of ours. That could be used as a test or a guide to find the solution.

We express our gratitude to the organizers of the workshop on Random Geometry Krakow 2003 for a most enjoyable atmosphere and hospitality. I would like to thank A. Dominguez and L. Tagliacozzo for interesting discussions and encouragement. The research contained in this talk is supported by the European Network EUROGRID and for a CIRIT grant 2001FI-00387.

Appendix A

Finding the B matrix propagator

To find the propagator we begin with the free action and add an external source. In our case this will lead to

$$\mathrm{Tr}\,[BMB + JB]\,. \tag{A.1}$$

Then, to reabsorb the external field J into the B field we do a linear change of variables $B \to \tilde{B} + C$ and quadratize the action. Doing the inverse procedure we find

$$\begin{aligned} \tilde{B}M\tilde{B} - CMC &= (B-C)M(B-C) - CMC \\ &= BMB - (CMB + BMC) = BMB - JB\,. \end{aligned}$$

So at the end the integral is

$$\begin{aligned} \tilde{Z}(J,M) &= \int dB\ \exp\{-\mathrm{Tr}[BMB - JB]\} \\ &= \Big(\det[M]\Big)^{-1}\ \exp\{\mathrm{Tr}[CMC]\}\,, \end{aligned} \tag{A.2}$$

where the C matrix can be determined from the equation

$$CM + MC = J\,. \tag{A.3}$$

Let us solve this equation to find the explicit form of the C matrix. To this aim let us choose the basis where the M matrix is diagonal. So if Ω is the matrix that diagonalizes it

$$\begin{aligned} M &= \Omega D \Omega^\dagger\,, \qquad \text{where} \qquad D_{ij} = \delta_{ij} d_i\,, \\ J &= \Omega J' \Omega^\dagger\,, \\ C &= \Omega C' \Omega^\dagger\,. \end{aligned} \tag{A.4}$$

The primed matrices correspond to the not primed ones after the rotation.

So now we will continue solving the equation (A.3) by writing it in the M-diagonal form,

$$\begin{aligned}(C'D + DC')_{ij} &= C'_{ij}d_j + d_iC'_{ij} = J'_{ij}\,,\\ C'_{ij} &= \frac{J'_{ij}}{d_i + d_j}\,.\end{aligned}$$

Now introduce it in Eq. (A.2) and invert Eq. (A.4) to find

$$\begin{aligned}Z(J,M) &= \Big(\det[M]\Big)^{-1}\ \exp\left\{\sum_{i,j=1}^{N}\left[\frac{J'_{ij}}{d_i+d_j}d_j\frac{J'_{ji}}{d_j+d_i}\right]\right\}\\ &= \Big(\det[M]\Big)^{-1}\exp\left\{\sum_{i,j=1}^{N}\frac{d_j}{(d_i+d_j)^2}[\Omega^\dagger_{ik}J_{kl}\Omega_{lj}][\Omega^\dagger_{jm}J_{mn}\Omega_{ni}]\right\}.\end{aligned}$$

That is the last expression we will write for $Z(J,M)$. From here we can deduce all necessary correlators, like the one we are looking for; the propagator $\langle B_{ij}B_{kl}\rangle = \delta Z(J,M)/\delta J_{ji}\delta J_{lk}\ |_{J=0}$. Calculating those variations and rotating back the D matrices we find

$$\begin{aligned}&Z(0,M)\left[\sum_{m,n=1}^{N}\frac{d_n}{d_m^2+d_n^2}\Big\{(\Omega^\dagger_{ml}\Omega_{kn})(\Omega^\dagger_{nj}\Omega_{im})+(\Omega^\dagger_{mj}\Omega_{in})(\Omega^\dagger_{nl}\Omega_{km})\Big\}\right]\\ &= Z(0,M)\left[\left[\frac{M\otimes\mathbb{I}}{[\mathbb{I}\otimes M + M\otimes\mathbb{I}]^2}\right]+\left[\frac{\mathbb{I}\otimes M}{[\mathbb{I}\otimes M + M\otimes\mathbb{I}]^2}\right]\right]_{il;kj}\\ &= Z(0,M)\left[\frac{\mathbb{I}\otimes\mathbb{I}}{\mathbb{I}\otimes M + M\otimes\mathbb{I}}\right]_{il;kj}.\end{aligned}\tag{A.5}$$

REFERENCES

[1] R.V. Ambartzumian, G.S. Sukasian, G.K. Savvidy, K.G. Savvidy, *Phys. Lett.* **B275**, 99 (1992); G.K. Savvidy, K.G. Savvidy, *Int. J. Mod. Phys.* **A8**, 3393 (1993); G.K. Savvidy, K.G. Savvidy, *Mod. Phys. Lett.* **A8**, 2963 (1993).

[2] G.K. Savvidy, F.J. Wegner, *Nucl. Phys.* **B413**, 605 (1994); G.K. Savvidy, K.G. Savvidy, *Phys. Lett.* **B324**, 72 (1994); G.K. Savvidy, K.G. Savvidy, F.J. Wegner, *Nucl. Phys.* **B443**, 565 (1995); J. Ambjorn, G. Koutsoumbas, G.K. Savvidy, *Europhys. Lett.* **46**, 319 (1999).

[3] G. Koutsoumbas, G.K. Savvidy, K.G. Savvidy, *Phys. Lett.* **B410**, 241 (1997).

[4] M. Baig, D. Espriu, D. Johnston, R.P.K.C. Malmini, *J. Phys. A: Math. Gen.* **30**, 7695 (1997).

[5] D. Espriu, M. Baig, D.A.Johnston, R.K.P.C. Malmini, *J. Phys. A: Math. Gen.* **30**, 405 (1997).

[6] D.A. Johnston, R.P.K. Malmini, *Phys. Lett.* **B378**, 87 (1996).

[7] A. Lipowski, D. Johnston, D. Espriu, *Phys. Rev.* **E62**, 3404 (2000).

[8] M.R. Swift, H. Bokil, R.D.M. Travasso, A.J. Bray, *Phys. Rev.* **B62**, 11494 (2000); `cond-mat/0003384`.

[9] A. Lipowski, *J. Phys. A: Math. Gen.* **30**, 7365 (1997).

[10] A. Lipowski, D. Johnston, `cond-mat/9812098`.

[11] A. Lipowski, D. Johnston, *Phys. Rev.* **E61**, 6375 (2000); A. Lipowski, D. Johnston, *Phys. Rev.* **E64**, 041605 (2001).

[12] P. Dimopoulos, D. Espriu, E. Jane, A. Prats, *Phys. Rev.* **E66**, 056112 (2002).

[13] G.K. Savvidy, `cond-mat/0003220`.

[14] G. Koutsoumbas, G.K. Savvidy, *Mod. Phys. Lett.* **A17**, 751 (2002).

[15] A. Barrat, R. Burioni, M. Mezard, *J. Phys. A: Math. Gen.* **29**, 1311 (1996).

[16] L. Chekhov, C. Kristjansen. *Nucl. Phys.* **B479**, 683 (1996); B. Eynard, C. Kristjansen, *Nucl. Phys.* **B516**, 529 (1998); I.K. Kostov, *Phys. Lett.* **B549**, 245 (2002).